

Topology Optimization of Simplified Actuating Structures subjected to Fluid-Structure Interaction by using the TOBS-GT Method

L. O. Siqueira¹, A. S. da C. Azevêdo¹, S. Ranjbarzadeh¹, E. C. N. Silva¹ and R. Picelli²

¹ Department of Mechatronics and Mechanical Systems Engineering, Polytechnic School of the University of São Paulo.

² Department of Naval Architecture and Ocean Engineering, Polytechnic School of the University of São Paulo.

Abstract. Over the years, interest in engineering has grown in materials that can recover and transform their shape. In this context, one of the challenges of topology optimization is to design structures built with these materials considering the rigor of their physics in the finite element procedure. This paper proposes a simplified approach to perform topology optimization of these actuating structures. The Topology Optimization of Binary Structures method with geometry trimming (TOBS-GT) is employed. In the TOBS-GT method, the finite element analysis and optimization modules are decoupled, where the geometry is updated and meshed freely in the FEA software. The structure is considered to actuate within a fluid flow domain, which requires a strongly coupled fluid-structure interaction analysis. The optimization of the actuator considers the minimization of the structural compliance subjected to a volume constraint. A body force is used to simulate an actuation on the structure and acts in the opposite direction to the fluid flow. The fluid flow is considered to be under low Reynolds regime. The algorithm is tested with a bidimensional example of a beam immersed in a fluid channel. The influence of body force variation on the final topology is tested. The results show that the TOBS-GT method can be used effectively to optimize structures subjected to fluid-structure interaction and a body force simultaneously.

Keywords: Topology Optimization, Integer Linear Programming, Body force, Actuator.

INTRODUCTION

Over the last few decades, topology optimization (TO) has gained ground in projects, replacing optimization tools such as shape or size. This growth is due to the advantages of TO over other approaches of optimization. From it, new holes can be introduced into the structure during optimization and it is generally not necessary to have a qualified initial guess to obtain projects with good performance (Lundgaard et al., 2018). In this way, TO has increasing application in several specialized and/or large production engineering fields, such as aerospace and automotive. However, despite this development, the optimization of multiphysics problems is still a big challenge. In this context, the problems of fluid-structure interaction stand out, which can be applied to important topics such as aeroelasticity, turbomachinery and offshore structures (Picelli et al., 2017).

Fluid-structure interaction (FSI) is a phenomenon that is present in our daily lives. In engineering problems, usually the effect of interaction of a fluid with a structure is neglected or simplified. However, in some cases, this effect can be extremely relevant and should not be ignored, for example, energy harvesters or actuators subject to fluid-structure interaction. In this specific type of problems, in addition to the difficulty already inherent in the fluid-structure interaction model, there is the difficulty of model the physics of this actuator device, which can be, for example, a material with shape memory alloy (SMA) or a piezoelectric (Tarek et al., 2012).

Seeking for sustainable alternatives, many researches have been focused on obtaining electrical energy from the ambient environment. Energy harvesters, usually made of piezoelectric material, take advantage of the piezoelectric effect is possible to absorb ambient energy, i.e., conversion of ambient mechanical energy to electrical energy. The cantilever beam is one of the most commonly type of used structures in piezoelectric energy harvesters for low frequency applications, especially in a fluid environment (Li et al., 2014; An et al., 2021). Elsewhere, SMA actuators are widely used in microcomponent and microdevice applications (Tarek et al., 2012). These materials can convert input electrical or thermal energy into output mechanical work, inducing system motion, producing high forces or large deformations, making them ideal as actuators. For this reason, SMA actuators have been considered for micropump actuations (Krondorfer et al., 2004; Teymouri and Sani, 2005; Krecinic et al., 2008; Zhu et al., 2009) where the stroke of the actuator determines the pumped volume per cycle (Tarek et al., 2012). In this work, aiming to simplify the finite element problem to perform topology optimization, the deformation caused in the structure by the piezoelectric effect or shape memory alloy effect will be simulated using a body force acting in fluid flow direction.

In the context of topology optimization of structures subject to fluid-structure interaction, there are still few studies

on the subject and each research uses a different approach to solve the problem. Yoon (2010) developed a monolithic approach to interpolate the governing fluid and structure equations using the SIMP (Solid Isotropic Material with Penalization) method. The same method was used to solve a stress-based problem subject to FSI (Yoon, 2014). Jenkins and Maute (2015) combined an explicit level set method (LSM) and the extended finite element method (XFEM) to optimize the internal layout of structures subjected to FSI considering large displacements. Jenkins and Maute (2016) developed a new approach to couple a Lagrangian formulation of the structure to an Eulerian fluid model, discretized on a deforming mesh using the level-set method to optimize structures subjected to FSI with design dependent loads considering large displacements. Furthermore, Picelli et al. (2017) modeled the structural and fluid domain with classical and separate governing equations to directly deal with the FSI problem using the BESO (Bi-directional Evolutionary Structural Optimization) method. Lundgaard et al. (2018) revisited the application of topology optimization using density methods (SIMP) for FSI. Picelli et al. (2020) developed a geometry trimming procedure to combine the integer linear programming (ILP) solver from TOBS with commercial finite element packages in fluid-structure interaction design with laminar flow. Recently, Ranjbardazeh et al. (2022) expanded the geometry trimming procedure created by Picelli et al. (2020) for the design of structures subject to fluid-structure interaction of a non-Newtonian fluid.

To our best knowledge, this is the first work to consider multiple loading in a fluid-structure interaction problem, i.e., fluid loading and body force acting in the structure simultaneously and considering large displacements. For this, it will be employed as optimization method the TOBS algorithm combined with the geometry trimming (TOBS-GT), using COMSOL Multiphysics as FEA solver. The TOBS-GT method is applied to design the two-dimensional (2D) wall in a channel under viscous fluid flow load and different values of body force acting in the direction of the fluid flow.

FLUID-STRUCTURE INTERACTION

Navier-Stokes Equations

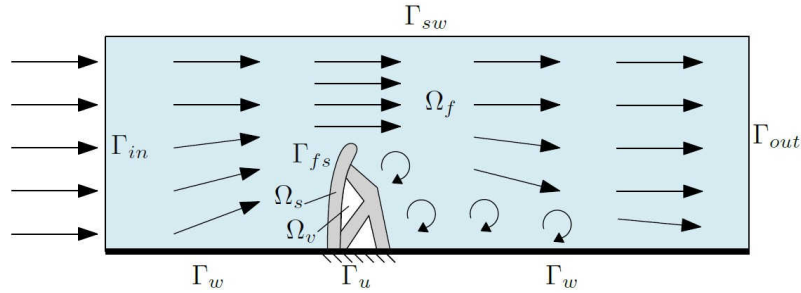


Figure 1 – Illustration of the FSI problem (Picelli et al. 2022).

The motion of a fluid particle in a fluid flow domain Ω_f , Fig. 1, is governed by the Navier Stokes and continuity equations (Paidoussis 1998). Considering a steadystate, incompressible, isothermal, and homogeneous fluid flow, with no body forces, the Navier-Stokes equation is given by:

$$\nabla \cdot (\mathbf{v}_f) = 0, \quad (1)$$

$$\rho_f (\mathbf{v}_f \cdot \nabla \mathbf{v}_f) = -\nabla P_f + \mu \nabla^2 \mathbf{v}_f \quad \text{on } \Omega_f, \quad (2)$$

where ρ_f is the fluid density, \mathbf{v}_f is the fluid velocity, μ is the fluid kinematic viscosity and P_f is the fluid pressure. Equation (1) refers to the fluid's incompressibility condition. Equation (2) corresponds to the momentum equation in a Eulerian formulation of reference. The terms on the left side of the equation are due to convective acceleration and the right side represents the internal forces in the fluid (inertial forces and viscous forces).

In order to solve the governing fluid equations, the following boundary conditions are imposed (Eqs. (3), (4) and (5)). The inlet flow condition is prescribed at the channel boundary Γ_{in} . A constrained pressure value at the outlet boundary Γ_{out} . A non-slip condition is imposed on the flow walls prescribed on the walls Γ_w and on the interface Γ_{fs} .

$$\mathbf{v} = \mathbf{v}_0 \quad \text{on } \Gamma_{in}, \quad (3)$$

$$P = p_0 \quad \text{on } \Gamma_{out}, \quad (4)$$

$$\mathbf{v} = 0 \quad \text{on } \Gamma_w \text{ and } \Gamma_{fs}, \quad (5)$$

Structural Analysis and Coupling

The total Lagrangian framework is used to describe the solid domain Ω_s in a Lagrangian frame. In Total Lagrangian framework, discrete equations are calculated with respect to the original configuration of the structure (undeformed position). Thus, the deformation gradient \mathbf{F} is expressed as

$$\mathbf{F} = \mathbf{I} + \nabla_u, \quad (6)$$

where \mathbf{I} is the unit diagonal matrix and ∇_u is the displacement gradient. The equilibrium state is described in terms of the 2nd Piola-Kirchhoff stress tensor as

$$\nabla \cdot (\mathbf{F} \cdot \mathbf{S}) = \mathbf{f}_{fsi}, \quad (7)$$

where \mathbf{S} is the 2nd Piola-Kirchhoff stress tensor and \mathbf{f}_{fsi} denotes the vector with the loads of the viscous fluid flow calculated at the interface Γ_{fs} . In order to solve Eq. (7), Dirichlet boundary conditions are applied at Γ_u as

$$\mathbf{u} = 0 \quad \text{on } \Gamma_u, \quad (8)$$

The coupling between solid domain and fluid domain at the FSI interface is defined by the kinematic and stress equilibrium conditions. The kinematic condition concerns the continuity in velocity and the stress equilibrium condition defines the continuity of the interface in the tractions (Lund et al, 2003). Thus, the coupling conditions for steady-state is expressed as

$$\boldsymbol{\sigma}_s \cdot \mathbf{n}_s = -\boldsymbol{\sigma}_f \cdot \mathbf{n}_f \quad \text{on } \Gamma_{fs}, \quad (9)$$

where $\boldsymbol{\sigma}_s$ is the solid stress tensor, $\boldsymbol{\sigma}_f$ is the fluid stress tensor, \mathbf{n}_s is normal unit vector outward to the solid and \mathbf{n}_f is normal unit vector outward to the fluid, both in the deformed configuration. Since small displacements are not considered, a moving mesh is used in order to evaluate the movement of the fluid-structure interface. In this case, occurs a two-way coupling, i.e., the fluid flow loads deforms the structure and the structure deformation changes the fluid domain changes due to the movement of the fluid-structure interface. The moving mesh interface in COMSOL Multiphysics employs the Arbitrary Lagrangian-Eulerian (ALE) method which separates the spatial frame (fluid domain) from the material frame (solid domain), enabling the easy identification of changes in physical boundaries.

TOPOLOGY OPTIMIZATION FRAMEWORK

Topology Optimization of Binary Structures

The TOBS method, proposed by Sivapuram and Picelli (2018), employs binary design variables $\{0,1\}$. This methodology linearizes the objective and constraint functions associated with integer linear programming (Williams, 2009). Therefore, the linearized optimization problem to be solved is given by:

$$\begin{aligned} & \text{Minimize} && \left. \frac{\partial f}{\partial \mathbf{x}} \right|_{\mathbf{x}^k} \Delta \mathbf{x}^k \\ & \text{Subject to} && \left. \frac{\partial g_i}{\partial \mathbf{x}} \right|_{\mathbf{x}^k} \Delta \mathbf{x}^k \leq \bar{g}_i - g_i^k \quad i \in [1, N_g] \\ & && \|\Delta \mathbf{x}^k\|_1 \leq \beta N_d \\ & && \Delta x_j \in \{-x_j, 1 - x_j\} \quad j \in [1, N_d] \end{aligned} \quad (10)$$

where $f(\mathbf{x})$ is the objective function, bounded by $g_i(\mathbf{x}) \leq \bar{g}_i$, $i \in [1, N_g]$, where N_g and N_d are respectively the number of inequality constraints and elements in the vector of design variables. β is the flip limits and $\|\Delta \mathbf{x}^k\|_1$ is the truncation error. The term g_i^k is the value of the constraint g_i in the k_{th} optimization iteration. The ILP solver is used to find the optimal change $\Delta \mathbf{x}$ for the integer design variables \mathbf{x} . After each iteration, the design variables are updated as $\mathbf{x}^{k+1} = \mathbf{x}^k + \Delta \mathbf{x}^k$.

Topology Optimization Problem

The formulation of the binary optimization problem from Eq. (10) is related to minimizing the mean compliance of the structure subject to a given volume and natural frequency constraints. The optimization problem is expressed as:

$$\begin{aligned}
 & \underset{x}{\text{Minimize}} && C(x) \\
 & \text{Subject to} && V_i(x) \leq \bar{V}_i, \quad i \in [1, N_g] \\
 & && x_j \in [0, 1], \quad j \in [1, N_d]
 \end{aligned} \tag{11}$$

where $C(x)$ is the structural compliance, V_i is the volume fraction of the structure and \bar{V}_i is the constrained volume fraction. The examples presented in this work are solved with one volume constraint, i.e., with $N_g = 1$.

Sensitivity Analysis

The TOBS is a gradient-based optimization method, hence the gradients (sensitivities) of the objective and constraint functions are required. A general way of calculate the sensitivities of a \mathbf{L} function is using the adjoint method (Haftka and Gurdal, 1991; Bendsoe and Sigmund, 2003). The general formulation of the adjoint equation for a Lagrangian functional can be given by

$$\left(\frac{\partial \mathbf{R}}{\partial u} \right)^T \lambda = - \left(\frac{\partial f}{\partial u} \right)^T, \tag{12}$$

where λ corresponds to the vector of adjoint variables, f is the vector of objective function and \mathbf{R} is the residual. Sensitivities can then be calculated by the following expression

$$\left(\frac{dL}{d\mathbf{x}} \right) = \left(\frac{\partial f}{\partial \mathbf{x}} \right)^T + \lambda^T \frac{\partial \mathbf{R}}{\partial \mathbf{x}}. \tag{13}$$

The structural mean compliance sensitivities are then calculated by the generic function, Eq. (13). The structural volume sensitivities with respect to the design variable x_j are expressed as

$$\frac{\partial V}{\partial x_j} = V_j, \tag{14}$$

where V_j is the volume fraction referring to the design variable x_j .

Material Model

In order to evaluate the derivatives of the structural compliance using the adjoint method via Eq. (13), the physical model should be interpolated with the design variables. We adopted the SIMP material model which is expressed as

$$E(x_j) = x_j^p E_0 \quad \text{on } \Omega_s, \tag{15}$$

where E is the interpolated material property with respect to the design variable x_j , E_0 is the Young's modulus of the solid element and p is the penalty exponent factor.

NUMERICAL IMPLEMENTATION

The TOBS-GT approach was developed by Picelli et al. (2020), that incorporates geometry trimming into the traditional TOBS method. Here, the material distribution method is based on the decoupling of the optimization and FEA module. The fluid-structure interaction and sensitivity analyses are solved and calculated using COMSOL Multiphysics and integer linear programming problem is solved using TOBS method. In general, the procedure is define an optimization grid defined as design domain and a binary topology (usually full solid). The contours of the void regions (holes) in the optimization grid are saved as .dxf CAD (computer-aided design) files for 2D problems. The contour information is then used to trim the initial design domain in the COMSOL Multiphysics. Holes that are located at the initial fluid-structure interfaces are then assigned to be filled with fluid. Figure 2 illustrates the TOBS-GT method.

The structural mean compliance is computed through the expression `solid.Ws_tot` incorporated in COMSOL Multiphysics. The sensitivities of the structural model are integrated in the variable `fsens(dtopol.theta_c)/dvol`, where `theta_c` is the vector of interpolation variables, Eq. (15). The sensitivities computed at each point are extracted through

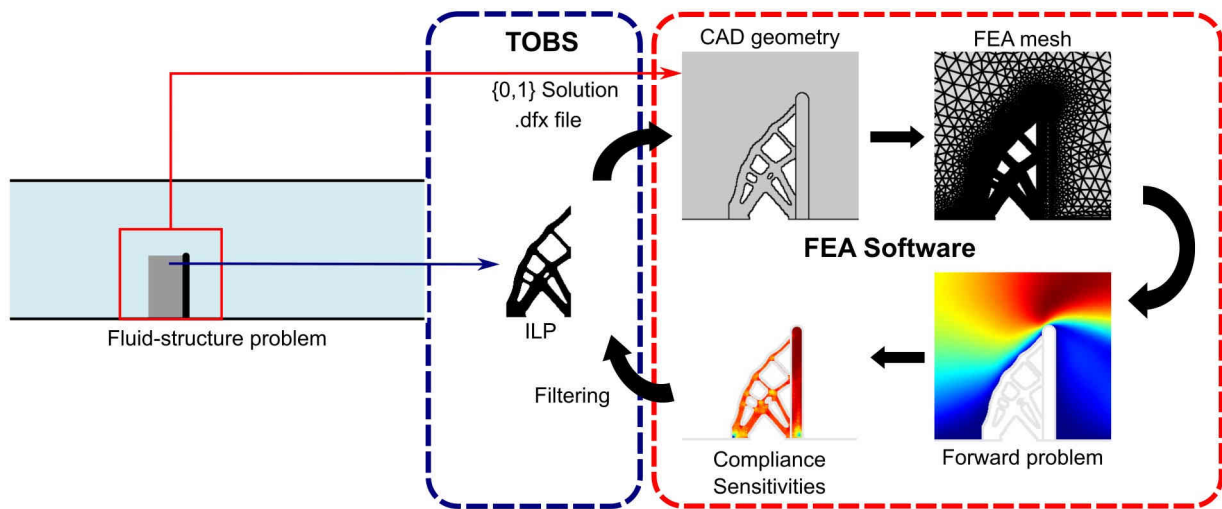


Figure 2 – Illustration of the complete optimization procedure.

a set of grid points coincident with the optimization grid. In the TOBS module, a numerical filter is applied to the sensitivities avoiding the well know checkerboard problem. With the respective sensitivities the optimizer provides a new set of binary variables $\{0, 1\}$. This process is repeated until convergence. A summary of the main steps for the TOBS-GT approach is presented below:

1. Define the TOBS parameters;
2. Create optimization grid and initialize design variables $\{0, 1\}$ in the TOBS module;
3. Generate a CAD geometry from contour and holes by reading the optimization grid variables;
4. Trim geometry with holes and create the fluid-structure topology in CAD;
5. Define fluid-structure interaction problem and mesh the geometry created by the CAD model;
6. Solve the FSI system governing equations;
7. Compute the automatic differentiated sensitivities in the grid points considering the mapping between the material and spatial frames;
8. Extract the calculated sensitivities in a grid coincident with the optimization grid;
9. Filter the sensitivity field defined in the grid points;
10. Solve the ILP problem and update the design variables $\{0, 1\}$ in the optimization grid;
11. Update design variables to build a new $\{0, 1\}$ topology;
12. If converged, stop. If not, iterate from step 3.

RESULTS AND DISCUSSION

This section presents the results obtained using the TOBS-GT method. The problem chosen for this analysis consists of a solid wall immersed in a fluid flow channel, Fig. 3. The goal the problem is to minimize the compliance of the structure subject to a volume fraction constraint of $V = 60\%$. A 50×500 optimization grid of quadrilateral elements is employed for optimization. A filter radius of 10 grid sizes is adopted. Material models are interpolated considering $p = 3$. The constraint relaxation parameter ϵ is set as 0.01, i.e., and the truncation parameter β is set as 0.04. In all the examples, the convergence is defined by averaging the changes in the compliance function over 6 consecutive iterations for a tolerance of $\tau = 0.001$.

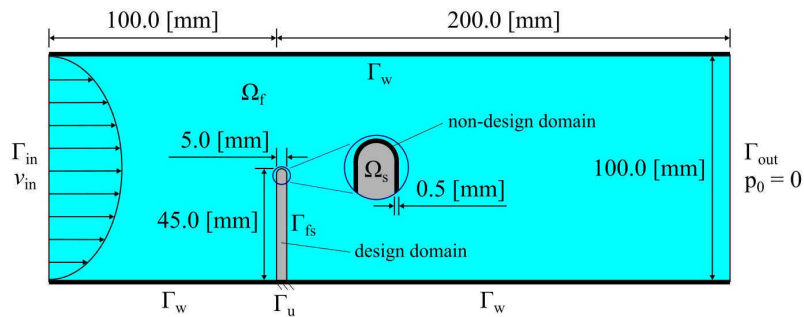


Figure 3 – Design domain for beam immersed in a fluid flow channel.

We seek to optimize the “dry” topology of the wall, i.e, the internal geometry. The properties of the solid material are Young’s modulus $E_0 = 2 \cdot 10^5$ Pa and Poisson’s ratio $\nu = 0.3$. The properties of fluid are density $\rho_f = 1000$ kg/m³ and dynamic viscosity $\mu = 1 \cdot 10^{-3}$ Pa · s. The average inlet velocity is defined by the Reynolds number described by $Re = \rho_f U_{in} D / \mu$, where U_{in} is the mean inlet velocity and D is channel height. Herein, we assume $Re = 100$. In all analysis the fluid flow is prescribed with a parabolic velocity profile at the channel inlet described by $\mathbf{v} = U_{in} 6(H - y)y / D^2$ where y is the coordinate in the y direction at each point of the inlet. A layer of passive elements with a thickness of 0.01 m is assumed between the interface and the design domain. The Fig. 4 presents the results of optimized structure and compliance history for different body force values [$B = 0, 100, 1000, 4000$ N/m³].

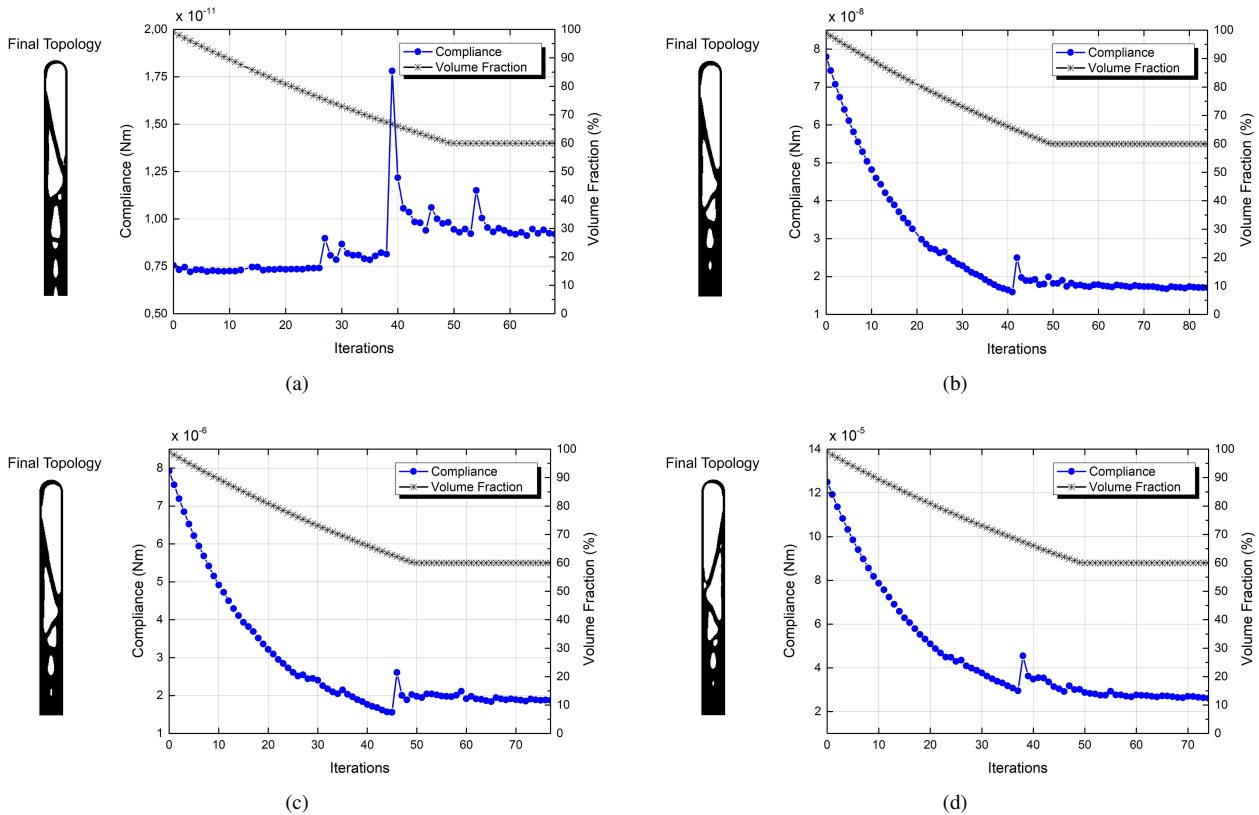


Figure 4 – Optimized structure and compliance history for different values of body force: (a) $B = 0$; (b) $B = 100$; (c) $B = 1000$; and (d) $B = 4000$.

Observing the topologies for all cases, it can be noted that the optimizer tends to concentrate a greater amount of material at the base of the structure in order to reduce overall deformations in the structure. In first case, which corresponds

only to fluid-structure interaction without the action of body force, we see that compliance tends to increase, Fig. 4(a). This occurs because of material removal and because there is no change in the fluid-structure interface, i.e., the load due to fluid flow remains constant during optimization. At another point, under conditions in which there is action of body force, compliance histories present similar behaviors, where compliance tends to decrease during optimization, Fig. 4(b), 4(c) and 4(d). This behavior is due to the removal of material from the structure, which implies a reduction in the total active body force. So, in this case we have that the body force tends to dominate the optimization. Fig. 5 presents the results of the velocity and pressure fields for the different body forces acting on the structure.

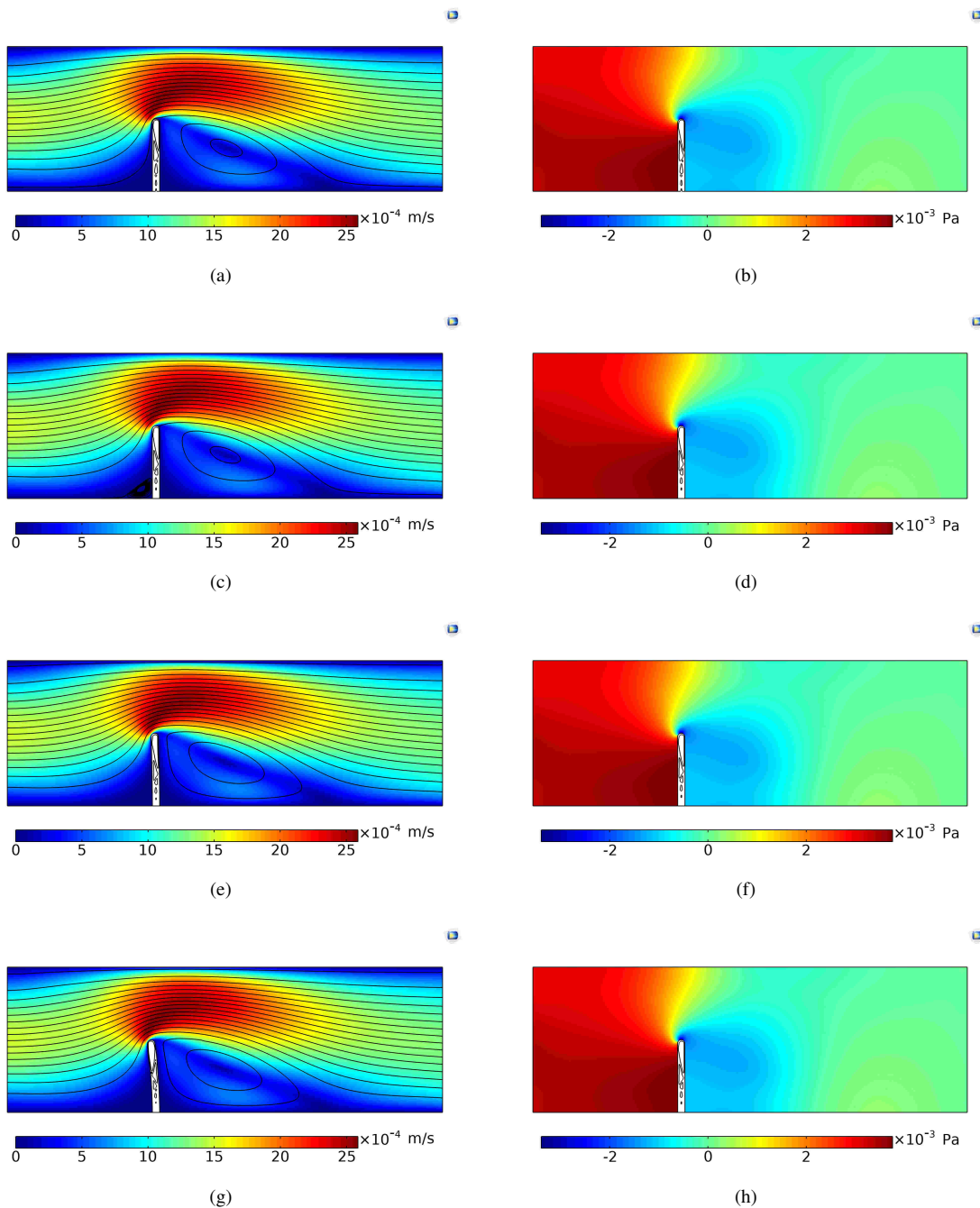


Figure 5 – Velocity field and Pressure for different values of body force: (a) B = 0, velocity field; (b) B = 0, pressure; (c) B = 100, velocity field; (d) B = 100, pressure; (e) B = 1000, velocity field; (f) B = 1000, pressure; (g) B = 4000, velocity field; and (h) B = 4000, pressure.

From the Fig. 5, it is observed that in the pressure field that there is a positive pressure field to the left of the structure and a small negative pressure field that forms well behind the structure. In a condition where forces due to fluid dominate, this pressure difference would cause the beam to shift to the right. Moreover, it is observed that even the condition with a body force of $B = 4000 \text{ N/m}^3$, Fig. 5(g), where there is a more visible displacement of the structure, does not cause a perceptible change in the fluid flow and in the pressure field. This must be because the generated velocities and pressures are very low, $25 \cdot 10^{-4} \text{ m/s}$ and $3 \cdot 10^{-3} \text{ Pa}$, which can cause large changes in flow. Finally, Fig. 6 shows the structure displacement fields with a scale factor of 4x.

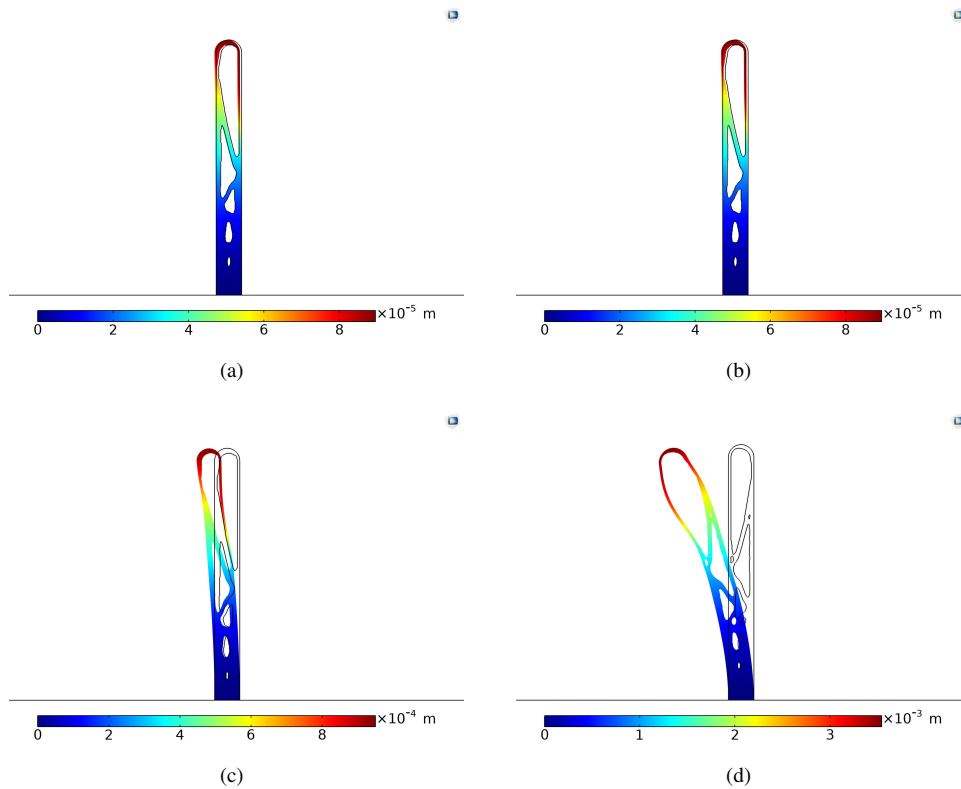


Figure 6 – Displacement field for different values of body force: (a) $B = 0$; (b) $B = 100$; (c) $B = 1000$; and (d) $B = 4000$.

Figure (6) shows the displacements caused by different body forces, simulating some type of action on the structure in the opposite direction to the flow. In practice, this action could correspond, for example, to a piezoelectric material subject to an electrical potential that causes a deformation in the body. For body force conditions equal to $B = 0 \text{ N/m}^3$ and $B = 100 \text{ N/m}^3$, the displacement is almost negligible, on the order of 10^{-7} and 10^{-5} m , respectively. For condition $B = 1000 \text{ N/m}^3$, the displacement amounts to approximately 1 mm and for condition $B = 4000 \text{ N/m}^3$, the displacement amounts to approximately 3.5 mm.

CONCLUSION

A study of topology optimization of minimizing compliance subject to a volume constraint of a structure subject to fluid-structure interaction and body force using TOBS method with geometry trimming. The results ensure that the method works efficiently working with viscous fluid flow load and body force acting simultaneously. The problem was solved for four different values of body force $B = 0, 100, 1000, 4000 \text{ N/m}^3$. For cases with body force, it was observed that the optimization of compliance minimization was dominated by body force. Thus, the behavior of the compliance history curve is the same for cases with body force, where compliance decreases because material removal reduces the total force acting on the structure.

ACKNOWLEDGMENTS

The first author thanks the financial support of FUSP (University of São Paulo Foundation) project number 371065 and FAPESP (São Paulo Research Foundation) under grant 2021/05930-2. The second author thanks the financial support of FUSP project number 371065. The third author thanks FAPESP under grant 2018/11474-7. The fourth author thanks the financial support of CNPq (National Council for Research and Development) under grant 302658/2018-1. The last author thanks FAPESP under the Young Investigators Awards program, grants 2018/05797-8 and 2019/01685-3. We gratefully acknowledge support of the RCGI – Research Centre for Greenhouse Gas Innovation, hosted by the University of São Paulo (USP) and sponsored by FAPESP – São Paulo Research Foundation (2014/50279-4 and 2020/15230-5) and Shell Brasil, and the strategic importance of the support given by ANP (Brazil’s National Oil, Natural Gas and Biofuels Agency) through the R&D levy regulation.

REFERENCES

- C. Lundgaard, J. Alexand, M. Zhou, C. Andreasen, and O. Sigmund. Revisiting density-based topology optimization for fluid-structure-interaction problems. *Structural and Multidisciplinary Optimization*, 58 (2018), 969-995.
- R. Picelli, W. M. Vicente, and R. Pavanello. Evolutionary topology optimization for structural compliance minimization considering design-dependent fsi loads. *Finite Elements in Analysis and Design*, 135 (2017), 44-55.
- Li, H., Tian, C., and Deng, Z. D. Energy harvesting from low frequency applications using piezoelectric materials. *Applied physics reviews*, 1 (4) (2014), 041301.
- An, X., Huang, H., Song, B. and Ma, C. Performance Evaluation of a Vortex Induced Piezoelectric Energy Converter (VIPEC) with CFD Approach. *Sustainability*, 13 (5) (2021), 2971.
- M. Tarek, A. Duval, and T. B. Zineb. Finite element analysis of a shape memory alloy actuator for a micropump. *Simulation Modelling Practice and Theory* 27 (2012): 112-126.
- R. Krondorfer, Y. K. Kim, J. Kim, C. G. Gustafson, T. C. Lommasson, Finite element simulation of package stress in transfer molded mems pressure sensors, *Microelectronics Reliability* 44 (12) (2004) 1995–2002.
- F. Krecinic, T. C. Duc, G. K. Lau, P. M. Sarro, Finite element modelling and experimental characterization of an electrothermally actuated silicon-polymer micro gripper, *Journal of Micromechanics and Microengineering* 18 (6) (2008)
- M. Zhu, P. Kirby, M. Wacklerle, M. Herz, M. Richter, Optimization design of multi-material micropump using finite element method, *Sensors and Actuators A* 149 (2009) 130–135.
- M. M. Teymoori, A. A. Sani, Design and simulation of a novel electrostatic micromachined pump for drug delivery applications, *Sensors and Actuators A* 117 (2005) 222–229.
- G. H. Yoon. Stress-based topology optimization method for steady-state fluid-structure interaction problems. *Computer Methods in Applied Mechanics and Engineering*, 278 (2014), 499-523.
- G. H. Yoon. Topology optimization for stationary fluid-structure interaction problems using a new monolithic formulation. *International Journal for Numerical Methods In Engineering*, 82 (2010), 591-616.
- N. Jenkins, K. Maute. Level set topology optimization of stationary fluid-structure interaction problems. *Structural and Multidisciplinary Optimization* 52 (1) (2015):179-195.
- N. Jenkins and K. Maute. An immersed boundary approach for shape and topology optimization of stationary fluid-structure interaction problems. *Structural and Multidisciplinary Optimization*, 54 (2016), 1191-1208.
- R. Picelli, S. Ranjbarzadeh, R. Sivapuram, R. S. Gioria, and E. C. N. Silva. Topology optimization of binary structures under design-dependent fluid-structure interaction loads. *Structural and Multidisciplinary Optimization*, 62 (2020), 2101-2116.
- S. Ranjbarzadeh, R. Picelli, R. Gioria, and E. C. N. Silva. Topology optimization of structures subject to non-Newtonian fluid–structure interaction loads using integer linear programming. *Finite Elements in Analysis and Design* 202 (2022), 103690.
- R. Sivapuram and R. Picelli. Topology optimization of binary structures using integer linear programming. *Finite Elements in Analysis and Design*, 139 (2018), 49-61.
- M. P. Paidoussis. *Fluid-structure interactions: slender structures and axial flow*, vol 1. Academic Press, 1998.
- E. Lund, H. Muller, L. Jakobsen. Shape design optimisation of stationary fluid-structure interaction problems with large displacement and turbulence. *Structural and Multidisciplinary Optimization* 25 (2003), 383-392.
- H. P. Williams. *Integer Programming, Logic and Integer Programming*. Springer US, Boston, MA, 2009.

R. T. Haftka, Z. Gurdal. Elements of Structural Optimization, 3rd edn. Kluwer Academic Publishers, 1991.

M. P. Bendsøe, O. Sigmund. Topology optimization - theory methods and applications. Springer, Berlin, 2003.

RESPONSIBILITY NOTICE

The author(s) is (are) the only party(ies) responsible for the printed material included in this paper.